International Journal of Fluid Machinery and Systems
Vol. 9, No.1, January-March 2016
DOI: http://dx.doi.org/10.5293/IJFMS.2016.9.1.085
ISSN (Online): 1882-9554

Original Paper

Unsteady Wet Steam Flow Measurements in a Low-Pressure Test Steam Turbine

Chongfei Duan[1], Koji Ishibashi[1], Shigeki Senoo[1]
Ilias Bosdas[2], Michel Mansour[2], Anestis I. Kalfas[3] and Reza S. Abhari[2]

[1]Turbo Machinery Research Department, Research & Development Center,
Mitsubishi Hitachi Power System, Ltd.
1-1, Saiwai-cho, 3-chome, Hitachi-city, Ibaraki, 317-0073 Japan,
chongfei_duan@mhps.com, koji_ishibashi@mhps.com, shigeki1_senoo@mhps.com
[2]Laboratory for Energy Conversion, Department of Mechanical and Process Engineering, ETH Zurich
IET, ML J 33, Sonneggstr, 3, CH-8092, Zurich, Switzerland
bosdas@lec.mavt.ethz.ch, michel.mansour@lec.mavt.ethz.ch, rabhari@lec.mavt.ethz.ch
[3]Department of Mechanical Engineering, Aristotle University of Thessaloniki
54124, Thessaloniki, Greece
anestis.kalfas@lec.mavt.ethz.ch

Abstract

An experimental study is conducted for unsteady wet steam flow in a four-stage low-pressure test steam turbine. The measurements are carried out at outlets of the last two stages by using a newly developed fast response aerodynamic probe. This FRAP-HTH probe (Fast Response Aerodynamic Probe – High Temperature Heated) has a miniature high-power cartridge heater with an active control system to heat the probe tip, allowing it to be applied to wet steam measurements. The phase-locked average results obtained with a sampling frequency of 200 kHz clarify the flow characteristics, such as the blade wakes and secondary vortexes, downstream from the individual rotational blades in the wet steam environment.

Keywords: Steam turbine, Wet steam, Unsteady flow measurement, Low-pressure stage

1. Introduction

Modern steam turbines are required to operate efficiently and safely over a wide range of operational states under various load conditions, such as a partial-load operation or a high back pressure condition [1]. As one of the effective measures for improving efficiency, to decrease the axial velocity of the last-stage outlet and reduce the emitted kinetic energy, development work aimed at increasing the size of the annulus area of the last stage has been done continuously [2]. With last-stage blade being longer, the flow structures, induced by the rotor-stator interaction and the unsteady pressure fluctuations at partial load, at the last two stages (L-1 stage and L-0 stage) would become more complex. Therefore, understanding the three-dimensional unsteady flow phenomenon is important to clarify the loss mechanism induced by the pressure fluctuation and to analyze the blade excitation for further improvement of reliability of steam turbines. For this purpose, many studies based on numerical simulations have been published (e.g. Senoo, et al. [3], Miyake et al. [4], Qi et al. [5]).

On the other hand, there is a considerable lack of time-resolved measurement data that have been obtained in the wet steam environment of low-pressure steam turbines owing to two major problems. One is damage or accuracy deterioration to the measurement devices caused by impinging and adhering droplets, and the other is the requirement for unsteady flow measurements to have a time resolution up to a sampling frequency of several hundred kHz.

In the conventional measurement technology, multi-hole pneumatic probes equipped with an air purging system are usually used for steady flow measurement in the wet steam environment of low-pressure steam turbines [6-7]. In order to clarify the relation between the unsteady flow field and the blade excitation, Shibukara et al. [8] used fast response pressure sensors to get a correlation between the vibration stresses of the last three stages and the pressure fluctuation in the flash-back steam. Segawa et al. [1] installed a Kulite pressure transducer on a probe, which can provide a 5 kHz sampling frequency, to measure the spanwise pressure fluctuations at the outlet of a moving blade in a low-pressure model steam turbine. Because of the lack of sufficient time resolution, the fluctuations of the

Received October 27 2015; accepted for publication December 18 2015: Review conducted by Tadashi Tanuma, Ph.D. (Paper number O15060S)
Corresponding author: Chongfei Duan, chongfei_duan@mhps.com

This paper was presented at 13th Asian International Conference on Fluid Machinery (AICFM), September 7-10, 2015, Tokyo, Japan

flow field were discussed based on the time-averaged results.

The purpose of this study is to investigate the unsteady phenomenon occurring at an individual rotational blade flow field in a wet environment. A newly developed FRAP-HTH probe (Fast Response Aerodynamic Probe – High Temperature Heated) is applied for unsteady measurement in a four-stage low-pressure test steam turbine. A miniature high-power cartridge heater is used to heat the probe tip to keep it clean of droplets [9]. FRAP-HTH results are validated by comparing to a 5-hole pneumatic probe (5HP) steady flow measurement results. In addition, the phase-locked average time resolved results obtained with a sampling frequency of 200 kHz provide detailed information at the individual rotational blade flow field.

2. Experimental Facility

All of the measurements presented in this paper are made in a four-stage (from L-3 to L-0 stages) low-pressure test steam turbine. A schematic diagram of the test facility and a photograph of the test turbine are shown in Fig. 1 and Fig. 2, respectively. The steam is generated by a boiler and the pressure and temperature are adjusted by a series of valves and desuperheaters. Then, the steam flows into the test turbine after passing through the main stop valve (MSV) and the control valve (CV). After passing through the turbine stages, the steam is condensed in a condenser and returned to the boiler finally. An orifice flowmeter is installed to measure the flow rate in the main steam pipe. A hydraulic dynamometer is connected to end of the turbine rotor and it absorbs the turbine-generated power. As shown in Fig. 3, single traverse measurements are performed at the downstream from the L-1 and L-0 stages. In order to compare the unsteady flow structures under various mass flow rates and backpressure conditions, three sets of measurements are conducted and the main parameters are summarized in Table 1. Since the test turbine is scaled by 1/2.2, the rotational speed is 7920 rpm. The numbers of the rotor blades are 96 and 70 for L-1 and L-0 stages, respectively. Therefore, by using the FRAP-HTH with the sampling frequency of 200 kHz, approximately 16 and 21 measured data can be acquired in one pitch downstream from the L-1 and L-0 stages, respectively, when a moving blade passes the fixed traversing position.

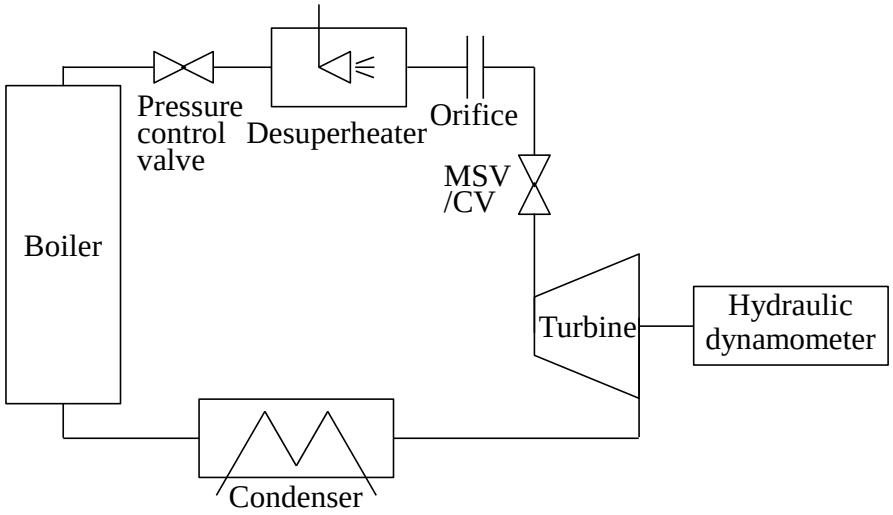

Fig. 1 Schematic diagram of test facility

Fig. 2 Photograph of the four-stage low-pressure test steam turbine

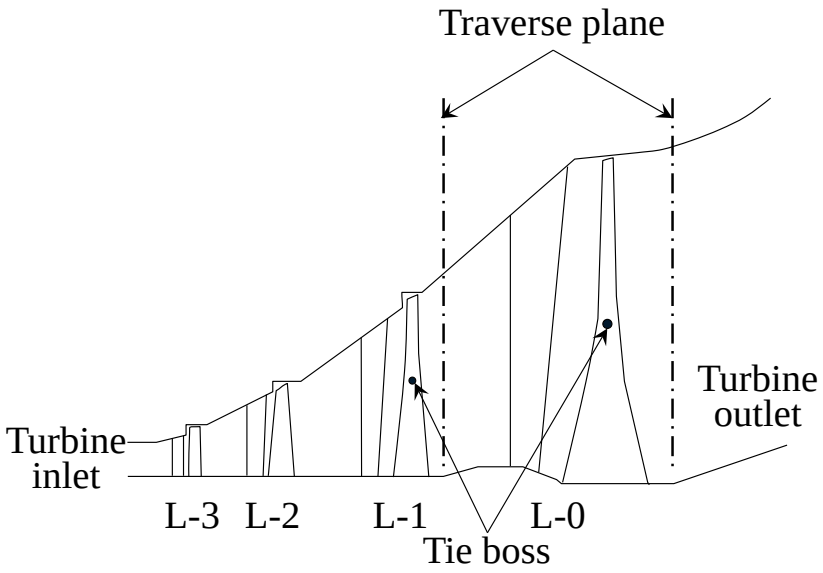

Fig. 3 Single-traverse measurement plane

Table 1 Measurement conditions

Condition	A	B	C	Unit
Mass flow rate	52	52	67	[t/h]
Vacuum condition	10.67	8.00	8.00	[kPa]
Turbine inlet temperature	266			[deg C]
Rotational speed	7920			[rpm]
Wetness fraction at L-1*	2.3	2.5	3.1	[%]
Wetness fraction at L-0*	4.5	6.5	8.0	[%]

*: Design value at pitch circle diameter

3. Measurement Instrumentations and Techniques

3.1 FRAP-HTH and 2-sensor probe in virtual 6-sensor mode measurement concept

The design and operation of the current fast-response aerodynamic probes are based on the developments made over the past two decades at the Laboratory for Energy Conversion at ETH Zürich [10-12]. The newly developed FRAP-HTH has some similarities to the probe developed by Lenherr et al. [11]. It has two piezo-resistive sensors encapsulated into the probe tip with 2.5 mm in diameter and can be operated to a temperature of 250 deg C.

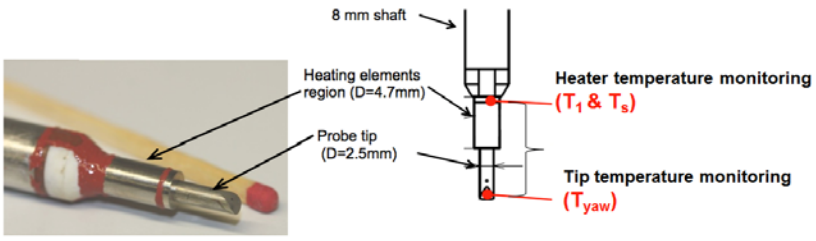

Fig. 4 FRAP-HTH probe schematic and temperature measurement locations [9]

In the present study, because the last two stages of the low-pressure test steam turbine operate in the wet steam environment, in order to remove the contamination of droplets to pressure taps, the probe tip is heated to several degrees above the maximum flow saturation temperature T_{sat} in the measurement plane. In addition, the FRAP-HTH is equipped with shielded pressure taps in order to protect the miniature piezo resistive sensors from direct droplet impacts [9]. As shown in Fig. 4, the probe tip is heated by a miniature high power density heater located close to the tip. The temperature of the probe tip is controlled by a PID regulator. The PID regulator adjusts the feeding current across the heater until the target temperature is reached. The temperature of the probe tip is kept constant during the traverse measurement. Basically, the tip temperature T_{tip} is defined as eq. (1).

$$T_{yaw} = T_{tip} = T_{sat} + \Delta T \tag{1}$$

3.2 2-sensor probe in virtual 6-sensor mode

The concept of the 2-sensor probe in the virtual 4-sensor mode was developed [11]. In the present low-pressure test steam turbine, because the flare angle is larger than 40 degrees in the last stage, the 2-sensor probe in the virtual 6-sensor mode is employed as shown in Fig. 5. In three consecutive steps, the first sensor is used to measure the actual pressures (p1, p2, p3) and the second sensor is used to measure the actual pressure (p4, p5, p6) at the roll angles set at 0, +42, and -42 deg, respectively. As shown in Table 2, these pressure values are then used for the definition of the different coefficients for flow yaw angle K_{yaw}, flow pitch angle K_{pitch}, total pressure K_{tot}, static pressure K_{stat}, as well as Mach number. The pressure data are checked independently in the post processing, and the different aerodynamic calibration coefficients are defined for the magnitude of the pitch incidence angles relative to the probe.

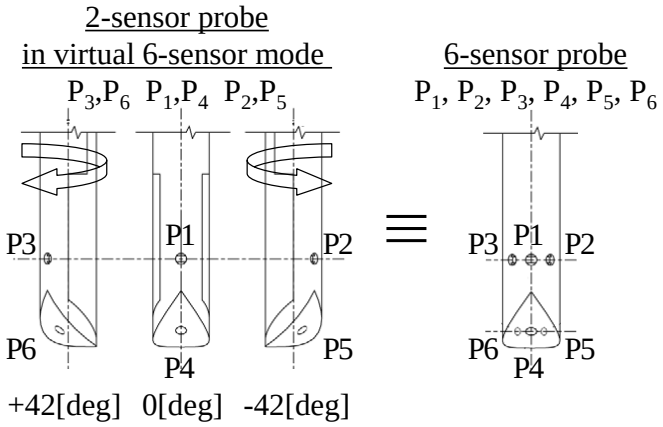

Fig. 5 2-sensor probe in virtual 6-sensor mode

Table 2 Extended aerodynamic calibration coefficients

Coefficients when $P_1 \geq P_4$	Coefficients when $P_4 < P_1$
$K_{yaw} = \frac{P_2 - P_3}{P_1 - \frac{(P_2 + P_3)}{2}}$	$K_{yaw} = \frac{P_5 - P_6}{P_4 - \frac{(P_5 + P_6)}{2}}$
$K_{pitch} = \frac{P_1 - P_4}{P_1 - \frac{(P_2 + P_3)}{2}}$	$K_{pitch} = \frac{P_5 - P_6}{P_4 - \frac{(P_5 + P_6)}{2}}$
$K_{total} = \frac{P_{total} - P_1}{P_1 - \frac{(P_2 + P_3)}{2}}$	$K_{total} = \frac{P_{total} - P_4}{P_4 - \frac{(P_5 + P_6)}{2}}$
$K_{stat} = \frac{P_{total} - P_{stat}}{P_1 - \frac{(P_2 + P_3)}{2}}$	$K_{stat} = \frac{P_{total} - P_{stat}}{P_4 - \frac{(P_5 + P_6)}{2}}$

3.3 Aerodynamic calibration and uncertainty

The aerodynamic calibration of the probe tip is performed in the fully automated free-jet facility at ETH Zürich. The probe is installed on a three-axis traversing system in order to rotate the probe relative to the fixed jet. The automatic calibration procedure follows a pre-defined measurement grid for different probe yaw angles and pitch angles [9]. As shown in Table 3, for the flow angle ranges and Mach number of interest, the polynomial curve-fit method of Gallington [13] is applied to the calibration data. In addition, similar to the analysis conducted by Behr [14], the whole chain of uncertainty sources is accounted for. That includes the uncertainties resulting from the calibration references and the polynomial interpolation curves of the calibration models, as well as the uncertainty sources related to the measurements. The resulting overall uncertainties are calculated using the Gaussian error propagation formula. The uncertainty calculation is performed using the GUM Workbench. Table 4 summarizes the respective measurement errors for the current average measurement conditions.

Table 3 FRAP-HTH calibration model accuracy for Ma=0.5 and calibration range of ±26 deg in yaw angle and -5 to 49 deg in pitch angle [9]

Parameter	Probe accuracy		Unit
	$P_1 \geq P_4$	$P_4 < P_1$	
Yaw angle	0.15	0.11	[deg]
Pitch angle	0.37	0.07	[deg]
Total pressure	122	38	[Pa]
Static pressure	288	103	[Pa]

Table 4 FPRA-HTH uncertainties calculated for the last stage conditions of the steam turbine test facility [9]

Parameter	Uncertainty	Unit
Yaw angle	0.27	[deg]
Pitch angle	0.75	[deg]
Total pressure	450	[Pa]
Static pressure	380	[Pa]
Mach number	0.12	[-]

4. Results And Discussion

In order to confirm the flow field conditions of measurement plane, the experiments started with 5HP traverse measurement with 11 radial points is conducted at L-1 and L-0 downstream. Then, in the same measurement plane, the FRAP-HTH traverse measurement is conducted with 33 and 31 radial points for L-1 and L-0 downstream, respectively. In this paper, the dimensionless results of total pressure, flow yaw angle and Mach number are discussed. The definition of the flow yaw angle is shown in Fig. 6.

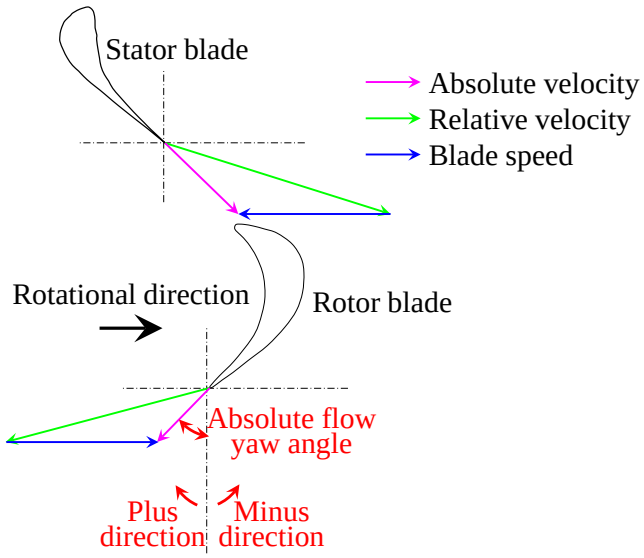

Fig. 6 Definition of flow yaw angle

4.1 Comparison of FRAP-HTH and 5HP time-averaged results

In order to validate the FRAP-HTH results, the time-averaged FRAP-HTH results (over 100 rotor revolutions for about 0.76 s) are compared to the 5HP steady flow measurement results (time-averaged data for 10 s by 1 Hz sampling rate). The results of total pressure (a), flow yaw angle (b), and Mach number (c), which are divided by the absolute values of the 5HP results at the PCD position for condition C, in L-1 and L-0 downstream are shown in Fig. 7 and Fig. 8, respectively. The FRAP-HTH time-averaged results (red line with rhombic marks), the instantaneous maximum values (long dashed line), minimum values (short dashed line), and 5HP steady measurement results (blue line with triangular marks) are plotted. In addition, the tie boss position is illustrated in the figures.

At L-1 downstream (Fig. 7), the time-averaged results of total pressure (a) show agreement between the two probes. In the time-averaged results of flow yaw angle (b), the tendency is similar and both probes capture the influence of the tie boss. However the flow yaw angle measured by the FRAP-HTH is larger than that measured by the 5HP probe. Two reasons for the difference of the flow yaw angles are considered. One is alignment error of the probes at their installation and the other is the flow angle detection error in the manual 5HP measurement. The time-averaged results of Mach number (c) show the same tendency for both probes, but the difference becomes slightly larger above a normalized blade height of 0.7.

At L-0 downstream (Fig. 8), all the results of both probes agree well for conditions A and B. There are small differences for condition C, because there is a time lag between the 5HP and FRAP-HTH measurements. The measurement plane at L-0 downstream is close to the exhaust hood, therefore a variation of the vacuum pressure directly affects static pressure at the exit of the L-0 stage. Since FRAP-HTH and 5HP time-averaged distributions in the radial direction show the similar tendency for all conditions, the newly developed FRAP-HTH can be used in the wet steam environment.

The FRAP-HTH instantaneous maximum and minimum values are also plotted in Figs. 7 and 8. It should be noted that the maximum and minimum values include instantaneous singular values. The ranges of unsteady fluctuations at L-1 downstream are larger than that at L-0 downstream because the distance between the rotational blade trailing edge and the measurement plane in the L-0 stage is approximately twice as long as that in the L-1 stage, and the swirl velocity in L-0 downstream is larger than that in L-1 downstream. These mean that the substantial distances between the rotational blade trailing edge and measurement points in L-0 are larger than in L-1. In addition, in the present measurement, several strain gauges are attached on the rotational blade surface to measure the vibrating stress. The strain gauges induce flow fluctuations. Since the number of rotational blades in the L-1 stage is larger than that in the L-0 stage, the relative volume of one strain gauge to one blade passage in the L-1 stage is larger than that in the L-0 stage. Therefore, the influences of the strain gauges in L-1 stage downstream are larger than that in L-0 stage downstream. As shown in Fig. 7 (c), larger maximum Mach numbers are found from the 80 % blade height to the tip. One reason for this is that the maximum value includes infrequent singular values.

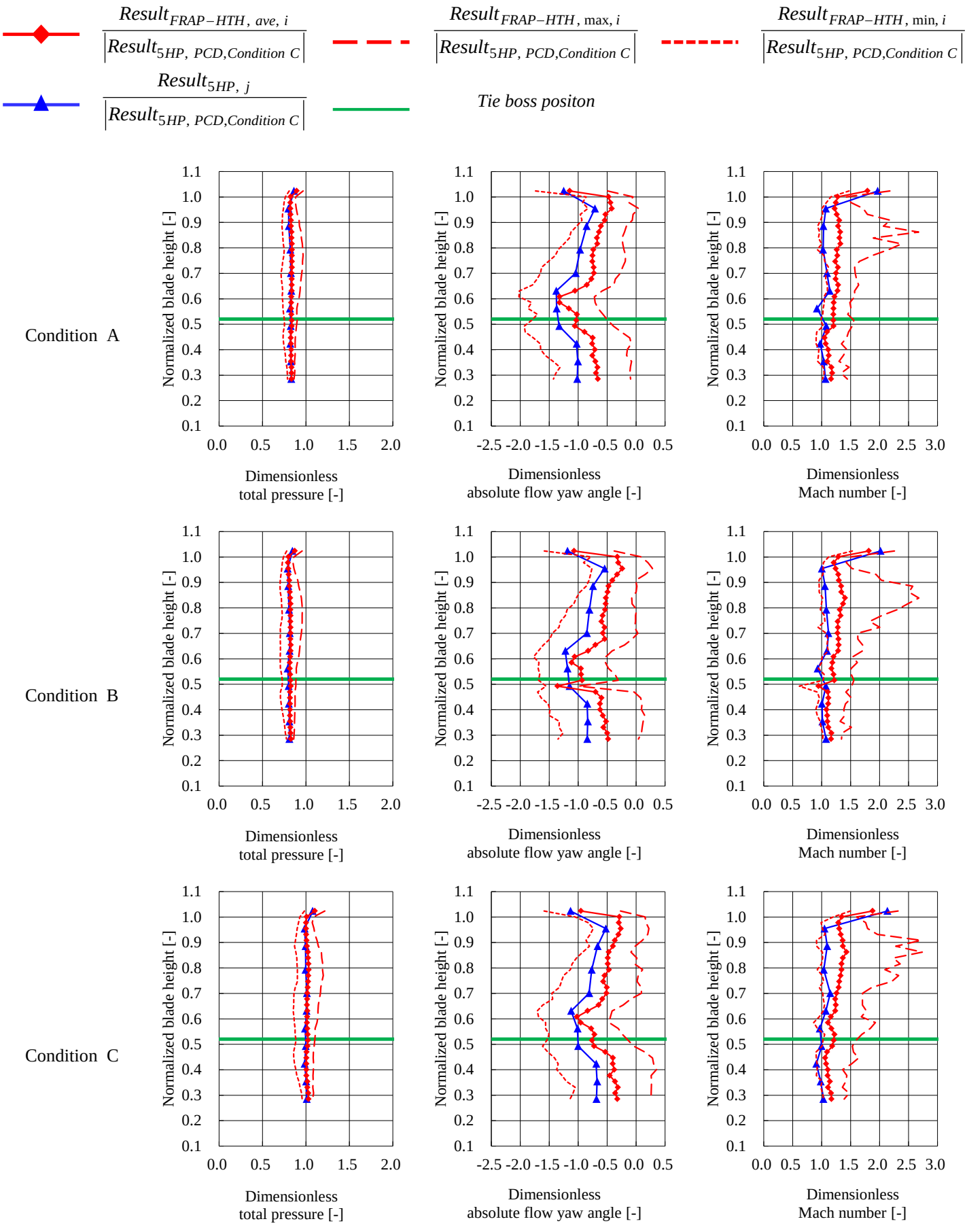

Fig. 7 Comparison of FRAP-HTH and 5HP results at L-1 downstream

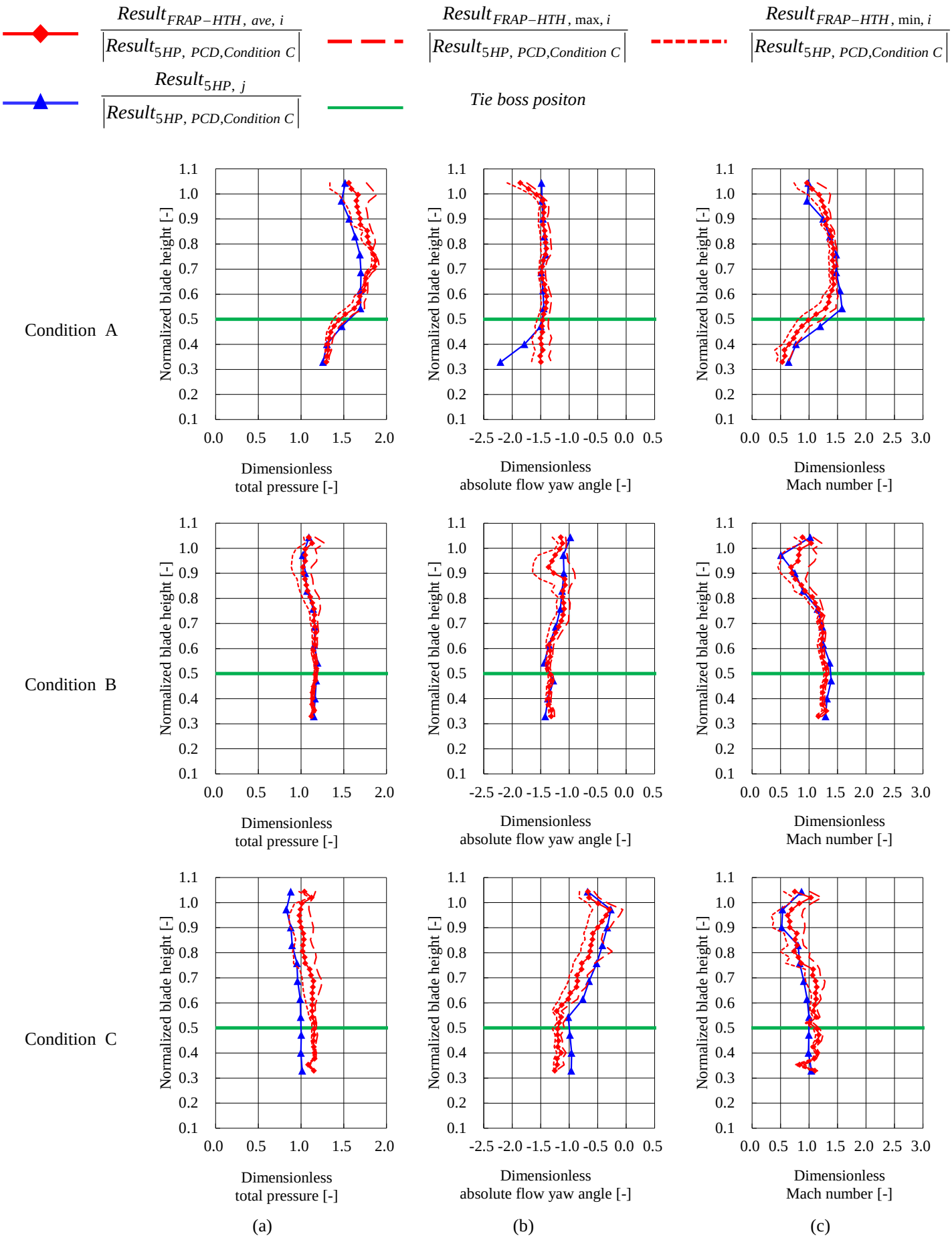

Fig. 8 Comparison of FRAP-HTH and 5HP results at L-0 downstream

4.2 Phase-locked time-resolved results

In order to investigate the flow field in an individual rotational blade, the phase-locked average method is applied. Since the measurement time is 2 s and the rotational speed is 132 rps, 264 rotor revolutions are recorded at every point. To find the appropriate number of rotor revolutions for the phase-locked average, the averaged results of different revolution numbers are compared. Here, 100 rotor revolutions are applied for the phase-locked average progress, since the phase-locked average results are not changed even if the average number of rotor revolutions is more than 100. In order to align the starting blade for the phase-locked average, an optical signal reflected from a narrow mark attacked on the shaft end is used as the trigger for the turbine rotation. The optical signals are also recorded by the FRAP-HTH measurement system with a 200 kHz sampling rate. Phase-locked average values of dimensionless total pressure and dimensionless absolute flow yaw angle are shown in Fig. 9 and Fig. 10 for L-1 and L-0 downstream, respectively. The values of the rotor blade passing period indicate the relative positions of the rotor blade to the position of the optical signal.

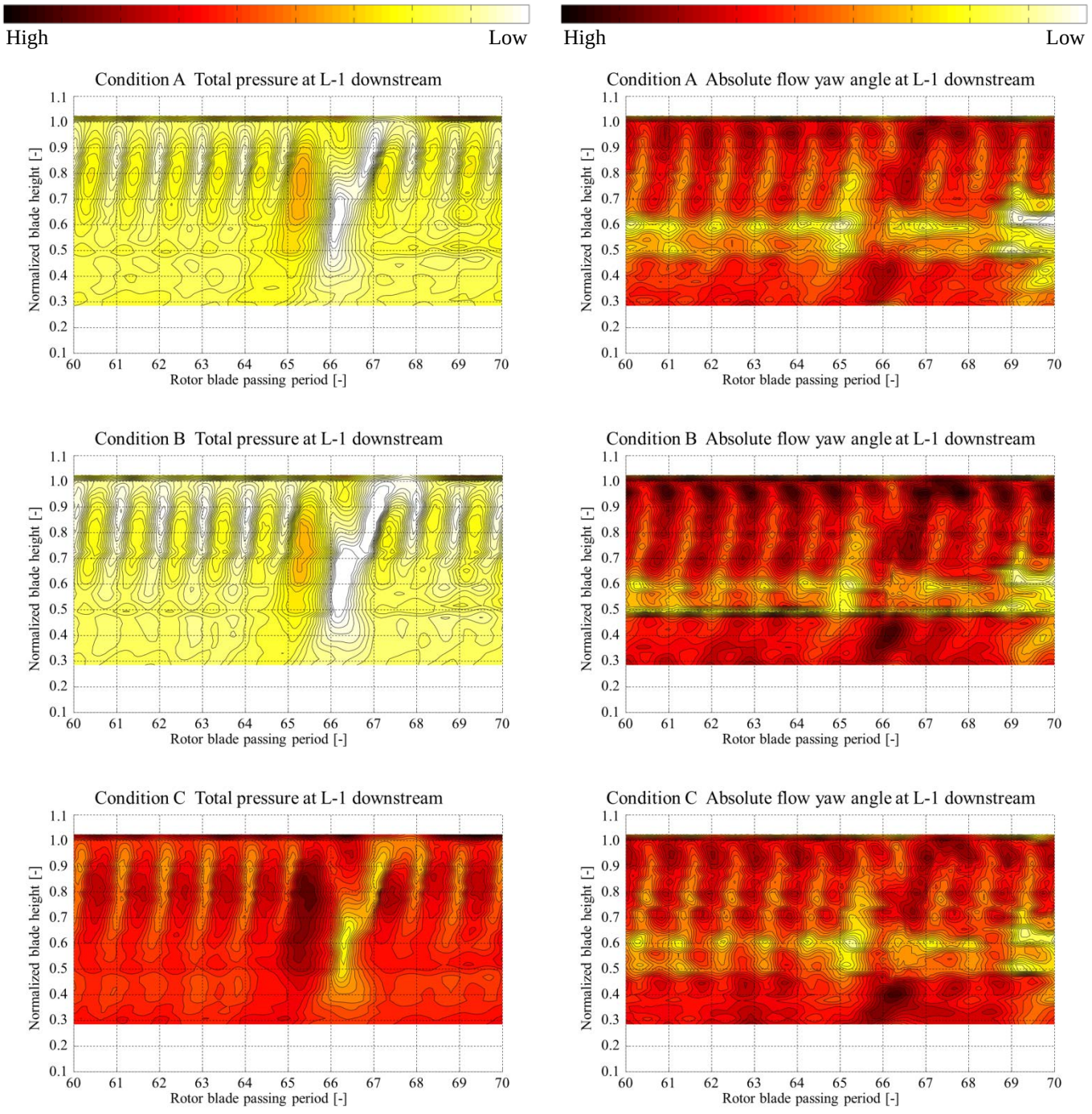

(a) Dimensionless total pressure (b) Dimensionless flow yaw angle

Fig. 9 Phase-locked average values in the rotational blades at L-1 downstream

At L-1 downstream, the FRAP-HTH clearly captures the periodic variations of total pressure and flow yaw angle induced by rotational blade wakes for the normalized blade height from 0.5 to 1.0. Near the tip, secondary vortexes are observed between wakes. The periodicity of the flow field is weakened due to the tie bosses located at the 0.5 blade height. In addition, the large fluctuations for rotor blade passing periods around 65 and 66 are induced by the strain gauge attached on the blade surface.

At L-0 downstream, the FRAP-HTH clearly captures the periodic variations of total pressure and flow yaw angle induced by rotational blade wakes for the normalized blade height from 0.7 to 1.0 and secondary vortexes near the tip. The larger distance between the rotor blade and the measurement plane and the large swirl angles weaken the periodicity below the 0.7 normalized blade height.

By using the FRAP-HTH with the sampling frequency of 200 kHz, approximately 16 and 21 measured data can be acquired in one pitch of L-1 and L-0 downstream respectively, when the moving blade passes the fixed traversing position. Based on such high time-resolution measurement technology, detailed phenomena can be investigated in wet steam environments.

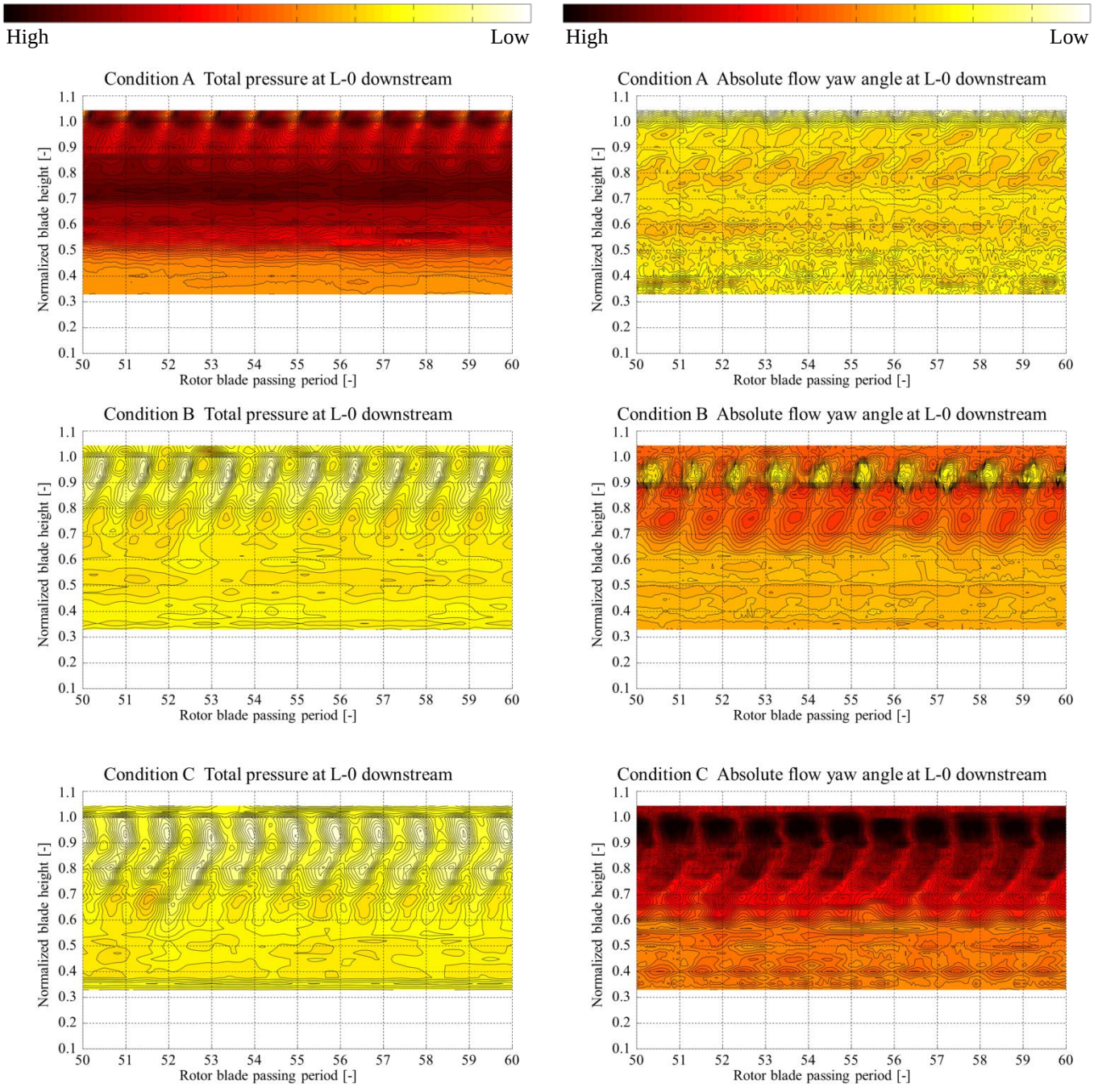

(a) Dimensionless total pressure

(b) Dimensionless flow yaw angle

Fig. 10 Phase-locked average values in the rotational blades at L-0 downstream

5. Conclusions

An experimental study was conducted for unsteady wet steam flow in a four-stage low-pressure test steam turbine. The unsteady data were obtained by using a newly developed FRAP-HTH. The FRAP-HTH has a miniature high-power cartridge heater with an active control system to heat the probe tip and keep it clean of droplets in the wet steam environment. The time-averaged results were validated by comparing with time-averaged results measured by a 5-hole pneumatic probe. The results indicate the FRAP-HTH can be used in the wet steam environment. The phase-locked average results obtained with the sampling frequency of 200 kHz were able to clarify the flow characteristics, such as blade wakes and secondary vortexes, downstream from individual rotational blades in the wet steam environment.

Nomenclature

K	Extended aerodynamic calibration coefficients [-]	T	Dimensionless total pressure [-]
P	Pressure [Pa]		

References

[1] Segawa, K., Senoo, S., Hamatake, H., Kudo, T., Nakamura, T., and Shibashita, N., 2012, "Steady and Unsteady Flow Measurements under Low Load Conditions in a Low Pressure Model Steam Turbine," ASME, Anaheim, California, ICONE20-POWER2012-54862.

[2] Senoo, S. and Ono, H., 2013, "Development of Design Method for Supersonic Turbine Aerofoils near the Tip of Long Blades in Steam Turbines, Part 2: Configuration Details and Validation," ASME Turbo Expo, San Antonio, Texas, USA, GT2013-94039.

[3] Senoo, S., Segawa, K., Hamatake, H., Kudo, T., Nakamura, T., and Shibashita, N., 2011, "Computations for Unsteady Compressible Flows in a Multistage Steam Turbine With Steam Properties at Low Load Operations," ASME Journal of Engineering for Gas Turbines and Power, Vol. 133, No. 10, 103001.

[4] Miyake, S., Koda, I., Yamamoto, S., Sasao, Y., Momma, K., Miyawaki T., and Ooyama H., 2014, "Unsteady Wake and Vortex Interactions in 3-D Steam Turbine Low Pressure Final Three Stage," ASME Turbo Expo, Düsseldorf, Germany, GT2014-25491.

[5] Qi, M., Yang, J., Yang, R., and Yang H., 2013, "Investigation on Loading Pulsation of LP Long Blade Stage in Steam Turbine," ASME Turbo Expo, San Antonio, Texas, USA, GT2013-94652.

[6] Miller, R. J., Moss, R. W., Ainsworth, R. W., and Horwood, C. K., 2003, "Time-Resolved Vane-Rotor Interaction in a High-Pressure Turbine Stage," Journal of Turbomachinery, Vol. 125, No. 1, pp. 1-13.

[7] Hodson, H. P. and Dawes, W. N., 1998, "On the Interpretation of Measured Profile Losses in Unsteady ‐ Turbine Blade Interaction Studies," Journal of Turbomachinery, Vol. 120, No. 2, pp. 276-284.

[8] Shibukawa, N., Iwasaki, Y., Takada, Y., Murakami, I., Suzuki, T., and Fukushima, T., 2014, "An Experimental Investigation of the Influence of Flash-back Flow on Last Three Stages of Low Pressure Steam Turbines," ASME Turbo Expo, Düsseldorf, Germany, GT2014-26897.

[9] Bosdas, I., Mansour, M., Kalfas, I. K., Abhari, R. S., and Senoo, S., 2015, "Unsteady Steam Flow Field Measurements in the Last Stage of Low Pressure Steam Turbine," ASME Turbo Expo, Montreal, Canada, GT2015-43504.

[10] Kuperfschmied, P., Köppel, P., Roduner, C., and Gyarmathy, G., 2000, "On the Development and Application of the FRAP (Fast-Response Aerodynamic Probe) System for Turbomachines – Part 1: The Measurement System," Journal of Turbomachinery, Vol. 122, No. 3, pp. 505-516.

[11] Lenherr, C., Kalfas, A. I., and Abhari, R. S., 2010, "High Temperature Fast Response Aerodynamic Probe," ASME Journal of Engineering for Gas Turbines and Power, Vol. 133, No. 1, 011603.

[12] Mansour, M., Kocer, G., Lenherr, C., Chokani, N., and Abhari, R. S., 2011, "Seven-Sensor Fast-Response Probe for Full-Scale Wind Turbine Flow Field Measurements," ASME Journal of Engineering for Gas Turbines and Power, Vol.133, No. 8, 081601.

[13] Gallington, R. W., 1980, "Measurement of Very Large Flow Angles With Non-Nulling Seven-Hole Probe," Aeronautics Digest, USAFA-TR-80-17, pp. 60-80.

[14] Behr, T., 2007, "Control of Rotor Tip Leakage and Secondary Flow by Casing Air Injection in Unshrouded Axial Turbine," Diss. ETH No. 17283.